J Biol Inorg Chem
DOI 10.1007/s00775-010-0749-4

ORIGINAL PAPER

Desulforubrerythrin from *Campylobacter jejuni*, a novel multidomain protein

Ana F. Pinto · Smilja Todorovic · Peter Hildebrandt · Manabu Yamazaki · Fumio Amano · Shizunobu Igimi · Célia V. Romão · Miguel Teixeira

Received: 10 September 2010 / Accepted: 1 December 2010

Abstract A novel multidomain metalloprotein from *Campylobacter jejuni* was overexpressed in *Escherichia coli*, purified, and extensively characterized. This protein is isolated as a homotetramer of 24-kDa monomers. According to the amino acid sequence, each monomer was predicted to contain three structural domains: an N-terminal desulforedoxin-like domain, followed by a four-helix bundle domain harboring a non-sulfur μ-oxo diiron center, and a rubredoxin-like domain at the C-terminus. The three predicted iron sites were shown to be present and were studied by a combination of UV–vis, EPR, and resonance Raman spectroscopies, which allowed the determination of the electronic and redox properties of each site. The protein contains two $FeCys_4$ centers with reduction potentials of +240 mV (desulforedoxin-like center) and +185 mV (rubredoxin-like center). These centers are in the high-spin configuration in the as-isolated ferric form. The protein further accommodates a μ-oxo-bridged diiron site with reduction potentials of +270 and +235 mV for the two sequential redox transitions. The protein is rapidly reoxidized by hydrogen peroxide and has a significant NADH-linked hydrogen peroxide reductase activity of 1.8 μmol H_2O_2 min^{-1} mg^{-1}. Owing to its building blocks and its homology to the rubrerythrin family, the protein is named desulforubrerythrin. It represents a novel example of the large diversity of the organization of domains exhibited by this enzyme family.

Keywords Rubrerythrin · Hydrogen peroxide · Rubredoxin · Electron paramagnetic resonance · Resonance Raman spectroscopy

Abbreviations

Ctb	*Campylobacter* truncated hemoglobin
Dps	DNA-binding protein from starved cells
DRbr	Desulforubrerythrin
Flrd-Red	NADH:flavorubredoxin oxidoreductase
FuR	Ferric uptake regulator
ICP	Inductively coupled plasma
KPi	Potassium phosphate
PerR	Peroxide regulator
rbo	Rubredoxin oxidoreductase
Rd-Flrd	Rubredoxin domain of flavorubredoxin
Rrc	Rubrerythrin-like protein from *Campylobacter jejuni*

Electronic supplementary material The online version of this article (doi:10.1007/s00775-010-0749-4) contains supplementary material, which is available to authorized users.

A. F. Pinto · S. Todorovic · C. V. Romão (✉) · M. Teixeira (✉)
Instituto de Tecnologia Química e Biológica,
Universidade Nova de Lisboa,
Avenida da República (EAN),
2780-157 Oeiras, Portugal
e-mail: cmromao@itqb.unl.pt

M. Teixeira
e-mail: miguel@itqb.unl.pt

P. Hildebrandt
Institut für Chemie,
Technische Universität Berlin,
Sekr. PC, 14, Str. des 17. Juni 135,
10623 Berlin, Germany

M. Yamazaki · S. Igimi
National Institute of Health Sciences,
1-18-1 Kamiyoga, Setagaya-ku,
Tokyo 158-8501, Japan

F. Amano
Osaka University of Pharmaceutical Sciences,
4-20-1 Nasahara, Takatsuki,
Osaka 569-1094, Japan

Published online: 19 December 2010

SDS-PAGE	Sodium dodecyl sulfate polyacrylamide gel electrophoresis
Tris	Tris(hydroxymethyl)aminomethane

Introduction

Campylobacter jejuni is a Gram-negative pathogenic proteobacterium of the epsilon group. It is the leading cause of food-borne diarrheal disease worldwide, having an infection dose as low as 500–800 bacteria; about two million cases per year of *C. jejuni*-associated gastroenteritis are estimated to occur just in the USA, and severer sequelae may occur subsequent to *C. jejuni* infection [1, 2]. *C. jejuni* colonizes the small bowel and the colon, where it finds a microaerobic environment. In fact, *C. jejuni* is only able to grow at low-oxygen partial pressures [3, 4]. The microaerobic lifestyle is made possible by a concerted interplay of oxygen-consuming enzymes (namely, the cbb_3-type oxygen reductase [5], which has a high oxygen affinity [6]) and oxidative-stress-responsive enzymes: microaerophiles such as *C. jejuni* are particularly vulnerable to the detrimental effects of oxidative stress and need to have efficient mechanisms to eliminate oxygen and its toxic species. Indeed, the genomes of *Campylobacter* species reveal the presence of genes coding for several of the canonical enzymes involved in detoxification of reactive oxygen species, such as catalase, superoxide dismutase, alkyl hydroperoxide reductase, *Campylobacter* truncated hemoglobin (Ctb), thiol peroxidase, DNA-binding protein from starved cells (Dps), and ferritin [7–10]. Some of these enzymes have been shown to be important for the colonization and persistence within macrophages [11, 12]. Apart from those enzymes, in recent years several novel systems involved in oxidative stress response have been described in anaerobes and microaerobes. Among them are the superoxide reductases and rubrerythrins [13, 14]. Whereas superoxide reductases directly eliminate the superoxide anion by its reduction to hydrogen peroxide, rubrerythrins have been proposed to eliminate hydrogen peroxide through its reduction to water. Rubrerythrins constitute a family of proteins with two types of iron sites: a non-sulfur diiron center of the μ-oxo-bridged histidine/carboxylate family, located in a four-helix-bundle structural domain, and a rubredoxin-type [$FeCys_4$] center, located at the C-terminal in most rubrerythrins. These proteins received this trivial name owing to the presence of the rubredoxin-like and hemerythrin-like diiron centers [15, 16]. Since the identification of the first rubrerythrin in the sulfate-reducing bacterium *Desulfovibrio vulgaris* [15], they have been found in the most diverse organisms of the three life domains, Archaea, Bacteria, and Eukarya [17–19]. Several physiological roles were proposed for these proteins, but the most consensual is hydrogen peroxide reduction, linked to NAD(P)H oxidation [20, 21]. Rubrerythrins have been found to complement catalase-null strains, and rubrerythrin-deletion mutants are more sensitive to oxygen and hydrogen peroxide [22]. In the genome of *C. jejuni* NCTC 11168 there is a gene, *cj0012c*, that encodes for a rubrerythrin-like protein [23]. This protein was identified by Yamasaki et al. [23] and they verified that the exposure of *C. jejuni* cell extracts to different concentrations of H_2O_2 led to the degradation of *Cj0012c*, suggesting that it is involved in the H_2O_2 oxidative stress response. A preliminary analysis of the deduced amino acid sequence suggested the presence of an additional domain at the N-terminus, apart from the rubrerythrin ones, namely, a putative desulfoferrodoxin-like domain, which led to the initially proposed name for this protein: rubredoxin oxidoreductase (rbo, the previous designation for desulfoferrodoxins)—rubrerythrin-like protein from *Campylobacter jejuni* (Rrc) [23]. Desulfoferrodoxins are 2Fe superoxide reductases, which have at the N-terminus a noncatalytic desulforedoxin-like domain [13]. Quite importantly, it was shown that the *cj0012c* gene was regulated by peroxide regulator (PerR) [12] as well as by ferric uptake regulator (Fur) [24, 25], which suggests its involvement in oxidative stress response as previously proposed [23]. Bacterial factors that combat reactive species enable the organisms to persist inside host cells, including macrophages, i.e., elucidation of oxidative stress responses is critical to understanding pathophysiological processes [4]. Therefore, we set out to extensively characterize this novel protein from *C. jejuni*, identify its three metal sites, and establish its in vitro function as an NADH-linked hydrogen peroxide reductase. Furthermore, owing to the unambiguous identification of each protein domain, we have renamed the protein desulforubrerythrin (DRbr) and will use this designation throughout the article.

Materials and methods

Expression of recombinant DRbr

The pMAL system (New England Biolabs) [26] was used for cloning the gene *cj0012c* from *C. jejuni* NCTC11168 as previously described [23] and was transformed into *Escherichia coli* strain BL21DE3 cells. Overexpression of DRbr was performed by growing this strain aerobically at 37 °C in M9 minimal medium, with 20 mM glucose, 400 μM $FeSO_4$, and 100 μg/ml ampicilin. When the optical density at 600 nm reached 0.3, isopropyl-1-thio-β-D-galactopyranoside was added (250 μM final concentration), and after approximately 16 h the cells were harvested by centrifugation, resuspended in a buffer containing 50 mM tris(hydroxymethyl)aminomethane (Tris)–HCl (pH 8), 100 mM NaCl, 1 mM $MgCl_2$, 0.1 mg/ml lysozyme, and

20 μg/ml DNase, and stored at −80 °C. The high amount of iron was essential to obtain the protein with the correct amount of iron incorporated.

Purification of recombinant DRbr

All purification procedures were carried out under anaerobic conditions at 4 °C, in a Coy glove box, with an O_2-free atmosphere constituted by a mixture of 95% argon and 5% hydrogen; all buffers were degassed and flushed with argon. The DRbr was followed throughout the purification procedure by sodium dodecyl sulfate polyacrylamide gel electrophoresis (SDS-PAGE) [27] and UV–vis spectroscopy. The soluble cellular extract was obtained after passing the cell suspension three times through a French press (35,000 psi), followed by ultracentrifugation at 125,000*g* for 1 h at 4 °C. It was subsequently applied onto a Q-Sepharose Fast Flow column (XK 26/10, GE Healthcare) previously equilibrated with 20 mM Tris–HCl (pH 7.2), and was eluted at 2 ml/min with a linear gradient from 0 to 1 M NaCl in the same buffer. The DRbr fraction which was eluted at approximately 0.2 M NaCl was then dialyzed overnight against 10 mM potassium phosphate (KPi) pH 7.0 buffer and loaded onto a Bio-Gel hydroxyapatite type II column (XK16/40, Bio-Rad), equilibrated with the same buffer. The protein was eluted with a linear gradient from 0 to 1 M KPi at pH 7.0. Fractions containing the protein were eluted at approximately 0.3 M KPi and were concentrated in a Diaflo ultrafiltration device (Amicon) using a YM10 membrane and applied to a molecular filtration column, Sephadex 75 (XK 26/60, GE Healthcare), equilibrated with 20 mM Tris–HCl (pH 7.2) and 150 mM NaCl. The final fraction was concentrated and its purity was verified by SDS-PAGE.

Determination of protein concentration, metal content, and molecular mass

The protein concentration was assayed by the bicinchoninic acid method [28], and the iron content was determined using 2,4,6-tripyridyl-1,2,3-triazine [29] and by inductively coupled plasma (ICP) emission spectrometry; the zinc content was also evaluated by ICP emission spectrometry. The molecular mass of the protein was determined by size-exclusion chromatography on a Superdex 200 column (XK 10/300, GE Healthcare), using appropriate molecular mass standards.

Sequence alignment and dendogram

Amino acid sequence alignments and dendrogram construction were performed with ClustalX [30] and GeneDoc [31] and the dendrogram was displayed with TreeView [32].

Spectroscopies

UV–vis spectra were acquired with a Shimadzu UV-1603 spectrophotometer; EPR spectra were collected with a Bruker EMX spectrometer, equipped with an ESR 900 continuous-flow helium cryostat from Oxford Instruments.

For resonance Raman studies, about 2 μl of 3 mM protein (in 20 mM Tris–HCl at pH 7.2) was introduced into a liquid-nitrogen-cooled cryostat (Linkam THMS600) mounted on a microscope stage and cooled to 83 K. Spectra of the frozen sample were collected in backscattering geometry using a confocal microscope coupled to the Raman spectrometer (Jobin Yvon U1000), and the 413-nm excitation line from a krypton ion laser (Coherent Innova 302). For isotopic labeling experiments, the protein was lyophilized and then redissolved in $H_2^{18}O$ or D_2O, and measured as described above. Typically, spectra were accumulated for 60 s with a laser power at the sample of 8 mW. After polynomial background subtraction, the frequencies and line widths of the Raman bands were determined.

Redox titrations

Redox titrations followed by EPR spectroscopy were performed anaerobically in 50 mM Tris–HCl (pH 7.2) at 25 °C, by stepwise addition of buffered (250 mM Tris–HCl at pH 9.0) sodium dithionite as a reductant or H_2O_2 as an oxidant. A 100 μM protein solution, platinum and Ag/AgCl electrodes, and the following redox mediators (40 μM each) were used: potassium ferricyanide ($E'^\circ = +430$ mV), *N*,*N*-dimethyl-*p*-phenylenediamine ($E'^\circ = +340$ mV), tetramethyl-*p*-phenylenediamine ($E'^\circ = +260$ mV), 1,2-naphthoquinone-4-sulfonic acid ($E'^\circ = +215$ mV), 1,2-naphthoquinone ($E'^\circ = +180$ mV), trimethylhydroquinone ($E'^\circ = +115$ mV), 1,4-naphthoquinone ($E'^\circ = +60$ mV), menadione ($E'^\circ = 0$ mV), plumbagin ($E'^\circ = -40$ mV), indigo trisulfonate ($E'^\circ = -70$ mV), phenazine ($E'^\circ = -125$ mV), 2-hydroxy-1,4-naphthoquinone ($E'^\circ = -152$ mV), and anthraquinone-2-sulfonate ($E'^\circ = -225$ mV). The electrodes were calibrated with a saturated quinhydrone solution at pH 7.0. The reduction potentials are reported with the standard hydrogen electrode as a reference. All experimental data were analyzed using Nernst equations for noninteracting redox centers considering single one-electron transitions for the rubredoxin and desulforedoxin domains, and two consecutive one-electron processes for the diiron center.

Peroxidase activities with artificial electron donors (*o*-dianisidine and guaiacol)

H_2O_2-dependent oxidation of *o*-dianisidine and guaiacol was followed at 460 and 470 nm, respectively, at room

temperature as a function of time in anaerobic conditions. For the two assays, 50 mM Tris–HCl pH 7.2 degassed under an argon flux was used and the final concentrations were as follows: 1 μM DRbr, 250 μM H_2O_2, and 1 mM *o*-dianisidine ($\varepsilon_{460} = 11.3$ mM^{-1} cm^{-1}), and 5 mM guaiacol ($\varepsilon_{470} = 26.6$ mM^{-1} cm^{-1}).

NADH-linked hydrogen peroxide reductase activity

As artificial electron-donating systems, a mixture of NADH:flavorubredoxin oxidoreductase (Flrd-Red) and the rubredoxin domain of flavorubredoxin (Rd-Flrd) [33], both from *E. coli,* were used. The *E. coli* proteins were purified as described in [33, 34]. The enzyme activity was measured anaerobically (under an argon atmosphere) at room temperature in 50 mM Tris–HCl (pH 7.2) in a closed spectrophotometric cell containing 150 μM NADH, 2 μM Flrd-Red, 4 μM Rd-Flrd, 200–500 nM DRbr, and 10 μM of H_2O_2. The NADH oxidation, initiated by addition of DRbr, was monitored by the decrease in absorbance at 340 nm ($\varepsilon = 6{,}220$ mM^{-1} cm^{-1}).

Results and discussion

Biochemical characterization

The DRbr was overexpressed in *E. coli*, grown in minimal medium supplemented with iron, and purified anaerobically through a three-step chromatographic process; from 1 l of culture medium approximately 60 mg of pure protein was obtained. The quantification of iron and zinc per mole of monomer gave 3.5 ± 0.2 and 0.17 ± 0.1, respectively, confirming that DRbr has approximately four iron atoms per monomer and virtually no zinc atoms.

By SDS-PAGE a single band at approximately 25 kDa was detected (Fig. S1), in agreement with the molecular mass deduced from the amino acid sequence, 24,526 Da. The elution profile in a gel filtration column revealed that the protein in solution is mainly in a form with a molecular mass of approximately 97 kDa, i.e., it forms a tetramer. Note that, in general, rubrerythrins are isolated as homodimers in solution [35, 36], whereas the X-ray structures of these proteins suggest either a dimeric or a tetrameric quaternary structure [35, 37, 38].

UV–vis spectra

The UV–vis spectrum of native (oxidized) DRbr (Fig. 1a, trace a) shows bands at 370, 490, and 560 nm, with an absorbance ratio A_{280}/A_{489} of 3.7. These features are reminiscent of [$FeCys_4$] ferric sites; diiron sites have, in general, low molar absorptivities, and so they are difficult to detect when in the presence of other chromophores. Figure 1b displays the spectra of a desulforedoxin-like center (Fig. 1b, trace a) and of a canonical rubredoxin (Fig. 1b, trace b). The addition of those two spectra in a 1:1 ratio (Fig. 1b, trace c) generates a spectrum with features almost identical to those of oxidized DRbr (Fig. 1b, trace d), including the relative absorbances at each maximum. In fact, the main difference between rubredoxin- and desulforedoxin-like sites resides in the relative absorbances of each main band: at 370 nm both iron centers have similar contributions, whereas at 490 nm, the spectral contribution of the rubredoxin site is approximately 50% higher than that of the desulforedoxin site. A deconvolution of the

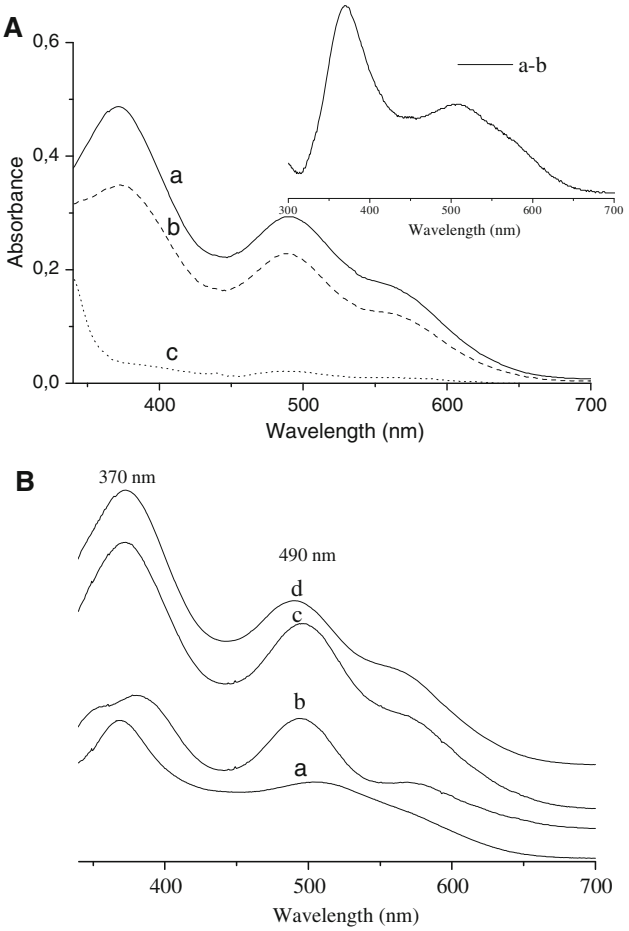

Fig. 1 UV–vis absorption spectra of *Campylobacter jejuni* desulforubrerythrin (DRbr). **a** Stepwise reduction of DRbr with sodium dithionite under anaerobic conditions: *a* spectrum of the as-isolated protein (50 μM) in 20 mM tris(hydroxymethyl)aminomethane (Tris)–HCl pH 7.2; *b* partially reduced protein after addition of substoichiometric amounts of sodium dithionite; *c* protein fully reduced by sodium dithionite; *inset* spectrum *a* minus spectrum *b*. **b** *a* Spectrum of partially reduced desulfoferrodoxin (Dx domain oxidized) from *Archaeoglobus fulgidus* [50]; *b* spectrum of *A. fulgidus* rubredoxin 1 [59]; *c* the 1:1 sum of spectra *a* and *b*; *d* spectrum of the as-isolated DRbr; the spectra are offset vertically and are displayed according to the respective molar extinction coefficients

components of the spectrum of the *C. jejuni* protein could be obtained after its partial reduction with sodium dithionite. Subtracting the spectrum of substoichiometrically reduced DRbr (Fig. 1b, trace b) from the spectrum of the oxidized form (Fig. 1a, trace a) reveals features identical to those of desulforedoxin (Fig. 1a, inset) [39], which further corroborates the presence of a rubredoxin site and a desulforedoxin site. Furthermore, the finding that the subtraction described yields the spectrum of a desulforedoxin indicates that this site has a reduction potential higher than that of the rubredoxin site. Complete reduction leads to the full bleaching of the visible absorption (Fig. 1a, trace c).

EPR spectra

The EPR spectrum at 7 K of the as-isolated DRbr (Fig. 2, trace a) displays several resonances at low magnetic fields, characteristic of high-spin ($S = 5/2$) ferric ions, and at g values slightly lower than 2, due to an $S = 1/2$ center. The resonances at low field could be deconvoluted into three distinct components, differing by the ratio of the zero-field splitting terms (rhombicity, E/D). By comparison with the corresponding g values of *D. gigas* desulforedoxin [39] and canonical rubredoxins (as well as of rubrerythrins) [40], the resonances due to the center with lower rhombicity ($E/D = 0.1$, $g = 8.0$ and $g = 3.6$ from the $|M_s = \pm 1/2>$ doublet and $g = 5.6$ from the $|M_s = \pm 3/2>$ doublet) can be assigned to the desulforedoxin-like center, whereas those with g values of 4.85 and 3.65 ($|M_s = \pm 3/2>$ doublet), and $g = 9.3$ (ground or excited doublet), are attributed to the rubredoxin-like center (with $E/D = 0.23$). This assignment is corroborated by the analysis of spectra obtained with partially reduced samples (Fig. 2, traces b and c), and taking into account that the desulforedoxin-like center is the one with the higher reduction potential. In fact, the first set of resonances to disappear from the spectra upon partial reduction are those of the spin system with $E/D = 0.1$. A third component is discernible in the spectra, with $g = 4.3$ and $E/D = 0.33$, which may be due to some heterogeneity at the ferric sites.

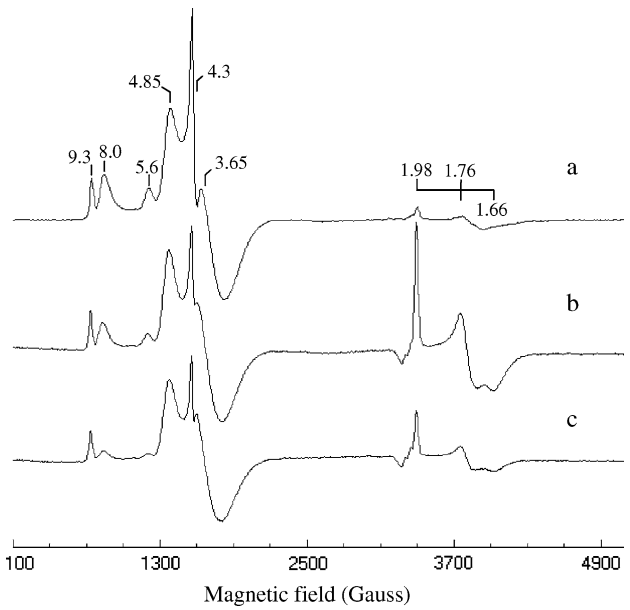

Fig. 2 EPR spectra of *C. jejuni* DRbr: *a* DRbr as isolated; *b* and *c* are spectra of DRbr upon successive addition of substoichiometric amounts of sodium ascorbate. The protein concentration was 200 μM in 20 mM Tris–HCl (pH 7.2) and 150 mM NaCl. Experimental conditions were as follows: 7 K; microwave power, 2 mW; microwave frequency, 9.38 GHz; modulation amplitude, 1 mT

The resonances with g values of 1.98, 1.76, and 1.66, better observed in a partially reduced state (Fig. 2, trace b), are detected up to approximately 20 K and are characteristic of an $S = 1/2$ center with antiferromagnetically coupled iron atoms in a mixed-valence (Fe^{III}–Fe^{II}) state [15, 41]. In the fully oxidized and reduced states, these resonances vanish (not shown), as characteristic of diiron centers of the histidine/carboxylate family, which form diferric or diferrous states with zero or even total spin [41]. No signals could be detected with parallel-mode EPR spectroscopy for either of those redox forms of the diiron center, which suggests either $S = 0$ total spin or a large value for the zero-field splitting.

Resonance Raman spectroscopy

The resonance Raman spectra of DRbr in the as-isolated state, obtained with 413-nm excitation, show several bands in the low-frequency region (Fig. 3, trace a). The bands at 316, 366, and 383 cm^{-1} are attributed to modes involving the Fe–S coordinates originating from both the rubredoxin and the desulforedoxin centers [41, 42]. In addition, a broad band at 520 cm^{-1} indicates the presence of an oxygen-bridged diiron center. This mode lies in the range of symmetric Fe–O–Fe stretching modes (ν_s) of μ-oxo-bridged diiron centers found in proteins and model complexes, and exhibits a large bandwidth as previously observed [43, 44]. The ν_s band is well defined in the spectra of ferricyanide-oxidized DRbr (data not shown) and H_2O_2-oxidized DRbr (Fig. 3, trace b). The assignment of the 520 cm^{-1} band is further supported by the results of isotopic labeling. For these experiments, the protein was lyophilized and then redissolved in $H_2^{18}O$ to substitute the bridging oxygen by ^{18}O [44–46]. The UV–vis absorption spectrum confirmed that the protein remained intact upon removal and subsequent addition of water (data not shown). As a consequence of the isotopic substitution, the 520 cm^{-1} band undergoes a downshift by approximately

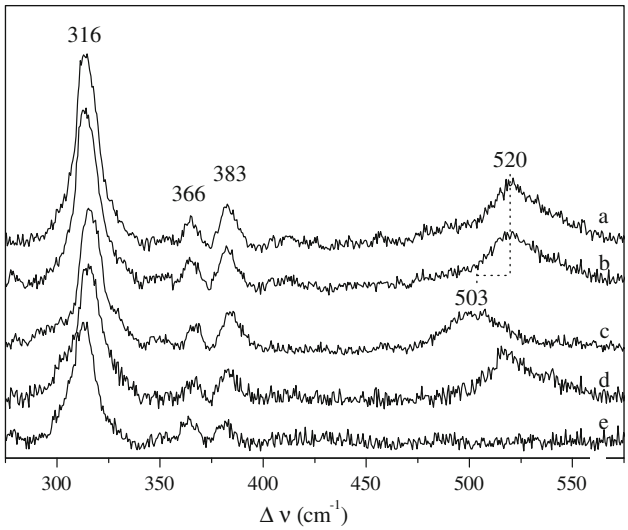

Fig. 3 Resonance Raman spectra of *C. jejuni* DRbr obtained with 413-nm excitation: *a* DRbr in the as-isolated state; *b* DRbr in the H_2O_2-oxidized state (essentially identical to the spectra of the ferricyanide-oxidized protein, data not shown); *c* DRbr in $H_2^{18}O$; *d* DRbr in D_2O; and *e* ascorbate-reduced DRbr. The spectra were measured at 83 K with an accumulation time of 60 s and a laser power at the sample of 8 mW

17 cm^{-1} to 503 cm^{-1} (Fig. 3, trace c). The magnitude of the $^{18}O/^{16}O$ shift of the ν_s mode ($\Delta\nu_s$) is characteristic of μ-oxo-bridged diiron centers [42, 44, 47, 48]. In particular, both the energy of the Fe–O–Fe stretching and the $^{18}O/^{16}O$ shift observed in DRbr are identical to the respective values reported for the diiron-oxo center in stearoyl–acyl carrier protein desaturase [44]. In that enzyme, the calculated Fe–O–Fe bond angle is 123°. Therefore, a similar value should hold for the DRbr diiron center, since there is a direct correlation of ν_s and $\Delta\nu_s$ with the geometry of the center. The subtle downshift of the band observed after dissolving the lyophilized protein in D_2O might reflect hydrogen-bonding interactions of the bridging oxygen but rules out the involvement of a hydroxyl ligand (Fig. 3, trace d).

Upon reduction of the protein with ascorbate, the 520 cm^{-1} band disappears. This finding can be readily attributed to the lack of resonance enhancement owing to the absence of an electronic transition in the ferrous form of the diiron center (Fig. 3, trace e). Note that $^{18}O/^{16}O$ and D/H exchange as well as reduction by ascorbate affect the vibrational modes of the rubredoxin and desulforedoxin centers only within the experimental accuracy (± 1 cm^{-1}).

Potentiometric characterization

The reduction potentials of each center were determined by redox titrations monitored by EPR spectroscopy. For the rubredoxin center (monitored at $g = 9.3$), a reduction potential of $+185 \pm 30$ mV was determined, whereas for the desulforedoxin center (monitored at $g = 8.0$ and $g = 5.6$), a value of $+240 \pm 30$ mV was obtained (Fig. 4a, c). For the diiron center, the changes in intensity at the $g = 1.76$ and $g = 1.66$ resonances were monitored. The bell-shaped data dependence was analyzed on the basis of a Nernst equation for two consecutive monoelectronic processes, yielding reduction potentials of $+270 \pm 20$ and $+235 \pm 20$ mV for the first (Fe^{III}–Fe^{III}/Fe^{III}–Fe^{II}) and second (Fe^{III}–Fe^{II}/Fe^{II}–Fe^{II}) steps, respectively.

The reduction potentials for the diiron center are within the values reported for the equivalent sites in rubrerythrins [41]. In contrast, the value determined for the desulforedoxin-like site, +240 mV, is quite high, as compared with the values of *D. gigas* desulforedoxin (−35 mV [49]) and of the desulforedoxin-like centers in desulfoferrodoxins (approximately 0 to −60 mV [50, 51]). In turn, the value obtained for the rubredoxin site, +185 mV, is lower than the values reported for the corresponding rubredoxin centers in rubrerythrins (+230 to +281 mV [15, 52]), but is still much higher than the values for isolated rubredoxins (generally, −100 to + 50 mV [40]). This observed difference may be partially explained by the presence of several amino acid substitutions in DRbr close to the iron-binding cysteines (vide infra).

$NADH:H_2O_2$ reductase activity

Having established the presence of the initially proposed metal centers, and determined their redox properties, we addressed the physiological role of *C. jejuni* DRbr.

Assays for peroxidase activity using as electron donors *o*-dianisidine and guaiacol in anaerobic conditions gave no activity. As observed for some rubrerythrins, DRbr is only slowly oxidized by oxygen, but rapidly (in the submillisecond range) by hydrogen peroxide (Fig. S2). The physiological electron donors of DRbr are not known, hampering a proper assay system for $NAD(P)H:H_2O_2$ oxidoreductase activity. Nevertheless, it was found that *E. coli* Flrd-Red was able to reduce DRbr in the presence of *E. coli* Rd-Flrd. Therefore, oxidation of NADH was monitored upon addition of H_2O_2 to a mixture containing catalytic amounts of Flrd-Red, Rd-Flrd, and DRbr (Fig. S3). An activity of 1.8 ± 0.4 μmol H_2O_2 min^{-1} mg^{-1} was obtained, which is similar to the values reported for other rubrerythrins, which range from 0.12 μmol H_2O_2 min^{-1} mg^{-1} for the *Entamoeba histolytica* enzyme [53] to 0.99 μmol H_2O_2 min^{-1} mg^{-1} for the *Clostridium acetobutylicum* protein [54]. Moreover, the NADH-to-H_2O_2 ratio was found to be 1 in the DRbr activity assays, which indicates that hydrogen peroxide was reduced to water. Therefore, we may conclude that, as rubrerythrins, *C. jejuni* DRbr has a role in detoxification of hydrogen peroxide.

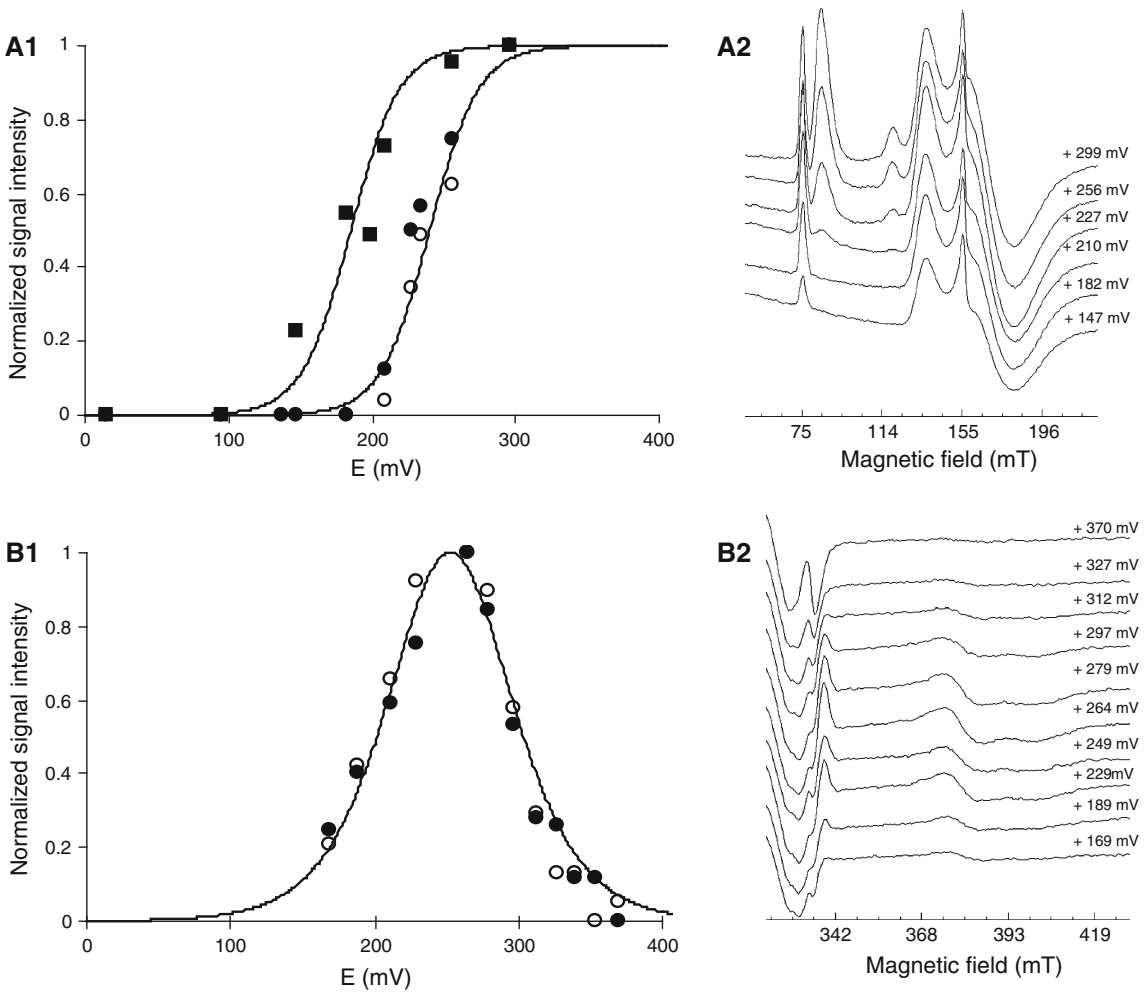

Fig. 4 Redox titration of DRbr, monitored by EPR spectroscopy. **a** Rubredoxin center, intensity changes of the $g = 9.3$ resonance (*squares*); desulforedoxin center, intensity changes of the $g = 5.6$ (*filled circles*) and $g = 8.0$ (*open circles*) resonances. The *solid lines* were calculated by Nernst equations for monoelectronic processes, with $E = +185$ mV and $E = +240$ mV. **b** EPR spectra of the redox titration of the rubredoxin and desulforedoxin centers at the potentials indicated. **c** Diiron center, intensity changes of the $g = 1.76$ (*filled circles*) and $g = 1.66$ (*open circles*) resonances; the *solid line* corresponds to a Nernst equation for two consecutive one-electron processes ($E_1 = +270$ and $E_2 = +235$ mV). The EPR signals were normalized in relation to the maximum intensity of each resonance. **d** EPR spectra of the redox titration of the diiron center at the potentials indicated

DRbr domains and sequence analysis

The amino acid sequences of *C. jejuni* DRbr and *D. vulgaris* rubrerythrin were used to search the sequence databases, from which 302 sequences of rubrerythrin-like homologous proteins were retrieved. These proteins are widespread in both prokaryotic domains, Archaea and Bacteria, in strictly anaerobic, facultative, or aerobic microorganisms and were also found in the genomes of eukaryotes such as the anaerobic protozoa *E. histolytica*, *Entamoeba dispar*, and *Trichomonas vaginalis*, and the photosynthetic protozoan *Cyanophora paradoxa*.

Analysis of the deduced sequences allowed us to establish that the large rubrerythrin family contains members composed of a quite diverse combination of four main types of structural domains: rubredoxin or desulforedoxin, four-helix bundle, and flavin reductase, as shown in Fig. S4. The distinctive feature of the family is the presence of the four-helix-bundle domain, harboring a diiron site and, thus, having the metal ligands conserved (see below). The simplest members of the family consist only of this domain, and were named erythrins [55], or, in the case of the protein isolated from *Sulfolobus tokodaii*, sulerythrin [56]. The rubredoxin and desulforedoxin domains are structurally similar, having in general two α-helices and two or three β-strands [40, 49], and harboring an iron coordinated by four cysteines, which acts as an electron transfer site. However, these two domains exhibit a major difference: in rubredoxins, the cysteines of the two pairs have two residues

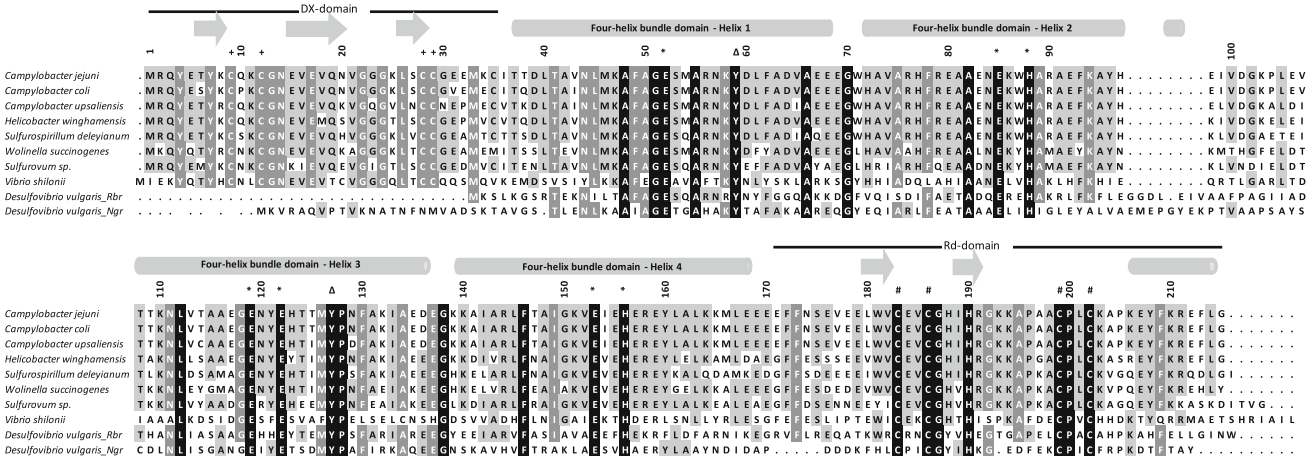

Fig. 5 Amino acid sequence alignment of the DRbr from *C. jejuni* subsp. *jejuni* NCTC 11168 with DRbrs identified so far in other organisms (percentage identity with *C. jejuni* subsp. *jejuni* NCTC 11168, NCBI-GI): *C. jejuni* subsp. *jejuni* NCTC 11168 (218561705); *C. coli* RM2228 (97%, 57504610); *C. upsaliensis* RM3195 (91%, 57505768); *Helicobacter winghamensis* ATCC BAA-430 (85%, 229376137); *Sulfurospirillum deleyianum* DSM 6946 (77%, 229532747); *Wolinella succinogenes* (71%, 34483443); *Sulfurovum* sp. NBC37-1 (68%, 151423895); *Vibrio shilonii* AK1 (34%,148837950); rubrerythrin from *Desulfovibrio vulgaris* Hildenborough (30%, 46581497) and nigerythrin from *D. vulgaris* Hildenborough (26%, 46578436). *Black* represents strictly conserved residues, *dark gray* represents highly conserved residues, and *light gray* indicates conserved residues among the sequences presented. *Plus signs* the N-terminal four cysteines corresponding to the Dx domain, *asterisks* the ligands involved in the diiron site, *triangles* tyrosine residues that form hydrogen bonds with two glutamate ligands, *hashes* the C-terminal four cysteines corresponding to the rubredoxin domain. The *top numbering* corresponds to the *C. jejuni* subsp. *jejuni* NCTC 11168 DRbr sequence

between them, C–$(X)_2$–C, whereas in desulforedoxins, the cysteines of the second pair are consecutive. The rubredoxin domains may appear at the N-terminus or at the C-terminus of rubrerythrins or even at both positions (see Fig. S4), whereas so far the desulforedoxin-like domain has been found only at the N-terminus. The rubredoxin domains from rubrerythrins can also be distinguished on the basis of the number of amino acids that separate the two pairs of cysteines: in most rubredoxin domains, this number is around 12, whereas in the equivalent domains from rubrerythrins from cyanobacteria and most isolated rubredoxins it is higher, about 30 amino acids, with the exception of the rubredoxin from *D. desulfuricans* ATCC 2774, which has 22. Another interesting difference between rubredoxin and desulforedoxin domains comes from their distribution: rubredoxins constitute, by themselves, a well-established family of proteins, widespread among prokaryotes and present also in a few eukaryotes, but may also appear as domains in several complex proteins, including the rubrerythrins or the flavorubredoxins [33]. In contrast, very few desulforedoxins are known; so far, only one protein has been purified, from *D. gigas* [39], and two orthologues were identified in the genomes of *Methanosarcina acetivorans* C2A and *Dehalococcoides* sp. CBDB1. Desulforedoxin-like domains are a fingerprint of the 2Fe superoxide reductases, or desulfoferrodoxins [13, 14, 50, 51].

A dendogram was built from the amino acid sequence alignment, using the neighbor-joining method available in Clustal X [30] (Fig. S4). Owing to the presence of different domains, the dendrogram was constructed taking into consideration only the amino acid sequence alignment of the common four-helix-bundle domain. The only well-defined monophyletic group in this dendogram is represented by the cyanobacteria. The remaining organisms, from the Bacteria, Archaea, and Eukarya domains, are scattered in the dendogram. The sequences cluster mainly according to the subfamilies of rubrerythrins, i.e., to the types of structural domains, although several exceptions were detected (not shown); in particular, the DRbrs form a separate cluster.

The amino acid sequence of *C. jejuni* DRbr corroborates the presence of three distinct metal sites from three different structural domains (Figs. 5, S4): (1) a desulforedoxin-like domain at the N-terminus, with a C–X_2–C–X_{15}–C–C motif, which precedes the rubrerythrin-like fingerprint, (2) a predicted four-helix-bundle domain, and (3) a subsequent rubredoxin-like domain, with a C–X_2–C–X_{12}–C–X_2–C motif at the C-terminus. DRbr is the first example of a characterized protein with the combination of these three structural domains, which is conserved in all *Campylobacter* species that have sequenced genomes (*C. coli* RM 2228, *C. lari* RM 2100, *C. upsaliensis* RM 3195, *C. hominis* ATCC BAA-381, and *C. concisus* 13826).

Genes encoding other orthologues were also found in other proteobacteria: *Helicobacter winghamensis*, *Sulfurospirillum deleyianum*, *Sulforuvum* sp., *Wolinella succinogenes*, and *Vibrio shilonii* (Fig. 5). The highest amino acid sequence identities and similarities of *C. jejuni* DRbr are with the orthologues from the same genus (approximately 90% identity) (Fig. 5). The proteins from *W. succinogenes* DSM 1740, *H. winghamensis*, and *S. deleyianum*, organisms that belong to the same order as *Campylobacter*, also have high identities and similarities with *C. jejuni* DRbr (approximately 70–85% identity). The average identity with rubrerythrins is 45–55%, with lower similarities with the "single domain" erythrin-like proteins.

It was concluded from the amino acid sequence alignment that all the amino acid residues involved as ligands of the binuclear center, on the four-helix bundle, and the four cysteines from the rubredoxin domain in the rubrerythrin family are strictly conserved in the DRbr sequences (Fig. 5): the ligands for the metal ions of the diiron site are E52–$(X)_{32}$–E85–$(X)_2$–H88–$(X)_{30}$–E119–$(X)_2$–E122–$(X)_{30}$–E153–$(X)_2$–H156 (numbering according to the *C. jejuni* DRbr); two tyrosines, whose homologues in the protein from *D. vulgaris* form hydrogen bonds with two glutamate ligands [38, 57]—Y59 (hydrogen bond with E119) and Y127 (hydrogen bond with E52), are also conserved; the binding motif for the rubredoxin domain is C183–$(X)_2$–C186–$(X)_{12}$–C199–$(X)_2$–C202.

The analysis of the amino acid sequences of the rubredoxin domains suggests a possible explanation for the lower reduction potential of the rubredoxin center of *C. jejuni* DRbr, in comparison with those from rubrerythrins. The high reduction potential of the rubredoxin site in rubrerythrins ($E_0 \sim +250$ mV) was attributed to the presence of a few amino acid substitutions in the cysteine binding loops, as compared with canonical rubredoxins, such as the *C. pasteurianum* protein ($E_0 = -57$ mV): the –CxVC– and –CpLCgV– motifs of this rubredoxin are substituted by –CxNC– and –CpACgH– in *D. vulgaris* rubrerythrin (Fig. 5) [57]. The presence of the asparagine and histidine residues changes the electrostatic environment near the iron ion, leading to an increase of the reduction potential [57, 58]. The sequence of *C. jejuni* DRbr shows the –CxVC– and –CpLCkA– motifs, i.e., it is more similar to that of *C. pasteurianum* rubredoxin than to the sequences of rubrerythrins. Interestingly, the motif found for *C. jejuni* DRbr is also present in all other DRbrs. Nevertheless, a detailed comparison of the electrostatics around the iron site can be made only once the three-dimensional structure of DRbr is available.

In summary, we have characterized a novel protein from the pathogen *C. jejuni*. It contains a distinct combination of structural modules: a desulforedoxin-like domain, a four-helix-bundle domain, and a rubredoxin-like domain. The presence of the latter two domains allows classification of the protein as a member of the large family of rubrerythrins. The combination of these three building blocks justifies the new name proposed for this protein, desulforubrerythrin (DRbr). The spectroscopic data show that the protein contains unequivocally two $FeCys_4$ centers (desulforedoxin- and rubredoxin-like) and a diiron center of the histidine/carboxylate type, with a μ-oxo bridge in the oxidized state.

We further showed that the protein has a hydrogen peroxide reductase activity, which agrees well with the fact that it is regulated by PerR and may play an important role in protection against oxidative stress conditions, contributing to sustaining the strict microaerophilic lifestyle of *C. jejuni*.

Acknowledgments This work was financed by Fundação para a Ciência e Tecnologia projects PDTC/BiaPro/67263/2006 (MT) and PDTC/BiaPro/67240/2006 (CVR). A.F.P. is recipient of the Ph.D. grant SFRH/BD/41355/2007. We thank Fay Mossel and João V. Rodrigues for their collaboration at early stages of this work. ICP emission spectrometry analyses were performed at the Laboratório de Análises (523-A), Departamento de Química, CQFB/REQUIMTE, FCT/UNL.

References

1. Poly F, Guerry P (2008) Curr Opin Gastroenterol 24:27–31
2. Young KT, Davis LM, Dirita VJ (2007) Nat Rev Microbiol 5:665–679
3. Bury-Mone S, Kaakoush NO, Asencio C, Megraud F, Thibonnier M, De Reuse H, Mendz GL (2006) Helicobacter 11:296–303
4. Fernie DS, Park RW (1977) J Med Microbiol 10:325–329
5. Weingarten RA, Grimes JL, Olson JW (2008) Appl Environ Microbiol 74:1367–1375
6. Jackson RJ, Elvers KT, Lee LJ, Gidley MD, Wainwright LM, Lightfoot J, Park SF, Poole RK (2007) J Bacteriol 189:1604–1615
7. Baillon ML, van Vliet AH, Ketley JM, Constantinidou C, Penn CW (1999) J Bacteriol 181:4798–4804
8. Day WA Jr, Sajecki JL, Pitts TM, Joens LA (2000) Infect Immun 68:6337–6345
9. Parkhill J, Wren BW, Mungall K, Ketley JM, Churcher C, Basham D, Chillingworth T, Davies RM, Feltwell T, Holroyd S, Jagels K, Karlyshev AV, Moule S, Pallen MJ, Penn CW, Quail MA, Rajandream MA, Rutherford KM, van Vliet AH, Whitehead S, Barrell BG (2000) Nature 403:665–668
10. Purdy D, Park SF (1994) Microbiology 140(5):1203–1208
11. Pesci EC, Cottle DL, Pickett CL (1994) Infect Immun 62:2687–2694
12. Palyada K, Sun YQ, Flint A, Butcher J, Naikare H, Stintzi A (2009) BMC Genomics 10:481
13. Pinto AF, Rodrigues JV, Teixeira M (2009) Biochim Biophys Acta 1804:285–297
14. Kurtz DM Jr (2006) J Inorg Biochem 100:679–693
15. LeGall J, Prickril BC, Moura I, Xavier AV, Moura JJ, Huynh BH (1988) Biochemistry 27:1636–1642
16. Klippenstein GL, Holleman JW, Klotz IM (1968) Biochemistry 7:3868–3878

17. Andrews SC (2010) Biochim Biophys Acta 1800:691–705
18. Putz S, Gelius-Dietrich G, Piotrowski M, Henze K (2005) Mol Biochem Parasitol 142:212–223
19. Weinberg MV, Jenney FE Jr, Cui X, Adams MW (2004) J Bacteriol 186:7888–7895
20. Coulter ED, Shenvi NV, Kurtz DM Jr (1999) Biochem Biophys Res Commun 255:317–323
21. Lumppio HL, Shenvi NV, Summers AO, Voordouw G, Kurtz DM Jr (2001) J Bacteriol 183:101–108
22. Sztukowska M, Bugno M, Potempa J, Travis J, Kurtz DM Jr (2002) Mol Microbiol 44:479–488
23. Yamasaki M, Igimi S, Katayama Y, Yamamoto S, Amano F (2004) FEMS Microbiol Lett 235:57–63
24. Palyada K, Threadgill D, Stintzi A (2004) J Bacteriol 186:4714–4729
25. Holmes K, Mulholland F, Pearson BM, Pin C, McNicholl-Kennedy J, Ketley JM, Wells JM (2005) Microbiology 151:243–257
26. http://www.neb.com/nebecomm/products/productE8000.asp
27. Laemmli UK (1970) Nature 227:680–685
28. Smith PK, Krohn RI, Hermanson GT, Mallia AK, Gartner FH, Provenzano MD, Fujimoto EK, Goeke NM, Olson BJ, Klenk DC (1985) Anal Biochem 150:76–85
29. Fischer DS, Price DC (1964) Clin Chem 10:21–31
30. Thompson JD, Gibson TJ, Higgins DG (2002) Curr Protoc Bioinformatics 2.3.1–2.3.22
31. Nicholas KB, Nicholas HB Jr, Deerfield DW II (1997) EMBnet.news 4(2):1–4
32. http://taxonomy.zoology.gla.ac.uk/rod/treeview.html
33. Gomes CM, Giuffre A, Forte E, Vicente JB, Saraiva LM, Brunori M, Teixeira M (2002) J Biol Chem 277:25273–25276
34. Gomes CM, Vicente JB, Wasserfallen A, Teixeira M (2000) Biochemistry 39:16230–16237
35. Tempel W, Liu ZJ, Schubot FD, Shah A, Weinberg MV, Jenney FE Jr, Arendall WB 3rd, Adams MW, Richardson JS, Richardson DC, Rose JP, Wang BC (2004) Proteins 57:878–882
36. Das A, Coulter ED, Kurtz DM Jr, Ljungdahl LG (2001) J Bacteriol 183:1560–1567
37. Fushinobu S, Shoun H, Wakagi T (2003) Biochemistry 42:11707–11715
38. Jin S, Kurtz DM Jr, Liu ZJ, Rose J, Wang BC (2002) J Am Chem Soc 124:9845–9855
39. Moura I, Bruschi M, Le Gall J, Moura JJ, Xavier AV (1977) Biochem Biophys Res Commun 75:1037–1044
40. Messerschmidt A, Huber R, Wieghardt K, Poulos T (eds) (2001) Handbook of metalloproteins. Wiley, New York
41. Gupta N, Bonomi F, Kurtz DM Jr, Ravi N, Wang DL, Huynh BH (1995) Biochemistry 34:3310–3318
42. Dave BC, Czernuszewicz RS, Prickril BC, Kurtz DM Jr (1994) Biochemistry 33:3572–3576
43. Kurtz DM (1990) Chem Rev 90:585–606
44. Fox BG, Shanklin J, Ai J, Loehr TM, Sanders-Loehr J (1994) Biochemistry 33:12776–12786
45. Sanders-Loehr J, Wheeler WD, Shiemke AK, Averill BA, Loehr TM (1989) J Am Chem Soc 111:8084–8093
46. Ravi N, Prickril BC, Kurtz DM Jr, Huynh BH (1993) Biochemistry 32:8487–8491
47. Todorovic S, Justino MC, Wellenreuther G, Hildebrandt P, Murgida DH, Meyer-Klaucke W, Saraiva LM (2008) J Biol Inorg Chem 13:765–770
48. LT Shiemke AK, Sanders-Loehr J (1986) J Am Chem Soc 108:2437–2443
49. Archer M, Huber R, Tavares P, Moura I, Moura JJ, Carrondo MA, Sieker LC, LeGall J, Romao MJ (1995) J Mol Biol 251:690–702
50. Rodrigues JV, Saraiva LM, Abreu IA, Teixeira M, Cabelli DE (2007) J Biol Inorg Chem 12:248–256
51. Tavares P, Ravi N, Moura JJ, LeGall J, Huang YH, Crouse BR, Johnson MK, Huynh BH, Moura I (1994) J Biol Chem 269:10504–10510
52. Pierik AJ, Wolbert RB, Portier GL, Verhagen MF, Hagen WR (1993) Eur J Biochem 212:237–245
53. Maralikova B, Ali V, Nakada-Tsukui K, Nozaki T, van der Giezen M, Henze K, Tovar J (2010) Cell Microbiol 12:331–342
54. Riebe O, Fischer RJ, Wampler DA, Kurtz DM Jr, Bahl H (2009) Microbiology 155:16–24
55. Andrews SC (1998) Adv Microb Physiol 40:281–351
56. Wakagi T (2003) FEMS Microbiol Lett 222:33–37
57. deMare F, Kurtz DM Jr, Nordlund P (1996) Nat Struct Biol 3:539–546
58. Luo Y, Ergenekan CE, Fischer JT, Tan ML, Ichiye T (2010) Biophys J 98:560–568
59. Rodrigues JV, Abreu IA, Saraiva LM, Teixeira M (2005) Biochem Biophys Res Commun 329:1300–1305